

## Neuroprotective Role of Gnidiol in Attenuating Oxidative Stress and Microglial Activation in LPS-Induced Neuroinflammation Models

L. Jyothi Rani<sup>1</sup>, Zeba Siddiqui<sup>2</sup>, Krishana Kumar Sharma<sup>3\*</sup>, Hiralben Mehta<sup>4</sup>, Sudheer Manawadi<sup>5</sup>, A.H. kulkarni<sup>6</sup>, Raveen Chauhan<sup>7</sup>, Jaya Vasavi G<sup>8</sup>

<sup>1</sup>Department of Pharmaceutics, Mallareddy institute of Pharmaceutical Sciences, Mallareddy Vishwavidyapeeth, Maisammaguda, Dhulappally, Secunderabad, 500100.

<sup>2</sup>Amity Institute of Pharmacy, Amity University, Madhya Pradesh -474005.

<sup>3</sup>Department of Pharmacology, Teerthanker Mahaveer College of Pharmacy, Teerthanker Mahaveer University, Delhi Road, Nh 24, Bagadpur Moradabad, Uttar Pradesh, 244001.

<sup>4</sup>Department of Quality Assurance, Pharmacy, Parul Institute of Pharmacy and Research, Parul University, PO. Limda, Ta.: Waghodiya Gujarat India -391760.

<sup>5</sup>Department of Biotechnology, Government Science College (Autonomous) Hassan 573201.

<sup>6</sup>Department of Pharmacology, Srinath College of Pharmacy, bajaj Nagar, Waluj, Chh. Sambhajinagar 431136.

<sup>7</sup>School of Pharmaceutical Sciences, Shoolini University Solan, Himachal Pradesh 173229.

<sup>8</sup>Department of Pharmaceutics, School of Pharmaceutical Sciences Vels Institute of science, Technology & Advanced Studies Pallavaram, Chennai, Tamilnadu 600117

### \*Corresponding Author:

Krishana Kumar Sharma

Email ID: [drkk108@gmail.com](mailto:drkk108@gmail.com)

### ABSTRACT

Neuroinflammation and oxidative stress are pivotal contributors to the progression of neurodegenerative diseases. This study investigated the neuroprotective potential of Gnidiol, a diterpenoid compound, in LPS-induced in vitro models of neuroinflammation using murine BV-2 microglial and human SH-SY5Y neuroblastoma cell lines. Treatment with lipopolysaccharide (1 µg/mL) significantly reduced cell viability, elevated reactive oxygen species (ROS), and increased the expression of pro-inflammatory cytokines (TNF-α, IL-1β, IL-6) along with microglial activation markers such as Iba1 and NF-κB. Pre-treatment with Gnidiol (1–25 µM) restored cell viability in a concentration-dependent manner and markedly reduced ROS levels and cytokine production. Immunocytochemical analysis revealed that Gnidiol suppressed NF-κB nuclear translocation and downregulated Iba1 expression, indicating a direct anti-inflammatory effect on activated microglia. The data suggest that Gnidiol exerts dual protective effects through attenuation of oxidative stress and inhibition of inflammatory signalling pathways. These findings support the therapeutic potential of Gnidiol as a neuroprotective agent and a candidate for further preclinical evaluation in neurodegenerative disease models characterized by chronic inflammation and oxidative stress.

**Keywords:** Gnidiol, Neuroinflammation, Oxidative stress, Microglial activation, NF-κB signalling, Neuroprotection.

**How to Cite:** L. Jyothi Rani, Zeba Siddiqui, Krishana Kumar Sharma, Hiralben Mehta, Sudheer Manawadi, A.H. kulkarni, Raveen Chauhan, Jaya Vasavi G, (2025) Neuroprotective Role of Gnidiol in Attenuating Oxidative Stress and Microglial Activation in LPS-Induced Neuroinflammation Models, *Journal of Carcinogenesis*, Vol.24, No.5s, 690-700

### 1. INTRODUCTION

Neuroinflammation and oxidative stress have emerged as key pathological features underpinning the onset and progression of various neurodegenerative disorders, including Alzheimer's disease, Parkinson's disease, multiple sclerosis, and amyotrophic lateral sclerosis. The central nervous system (CNS), despite being an immunoprivileged site, is not immune to immune-mediated damage. Microglial cells, the resident immune cells of the CNS, play a pivotal role in maintaining neural homeostasis. However, in response to harmful stimuli such as lipopolysaccharides (LPS), beta-amyloid, or environmental toxins, microglia undergo a phenotypic switch from a resting (M0) to an activated (M1) state. This transition

triggers the release of various pro-inflammatory cytokines (e.g., TNF- $\alpha$ , IL-1 $\beta$ , IL-6) and reactive oxygen species (ROS), thereby amplifying neuronal damage and dysfunction. Consequently, persistent microglial activation and sustained neuroinflammatory signaling are now considered central mechanisms contributing to neurodegeneration (Ansari *et al.*, 2022; Menghi *et al.*, 2023; Song *et al.*, 2021; Usui *et al.*, 2023).

Among the intracellular signalling cascades involved in this inflammatory response, the nuclear factor kappa-light-chain-enhancer of activated B cells (NF- $\kappa$ B) pathway is particularly noteworthy. NF- $\kappa$ B activation leads to the transcription of numerous pro-inflammatory genes and enzymes such as inducible nitric oxide synthase (iNOS) and cyclooxygenase-2 (COX-2). Similarly, oxidative stress resulting from mitochondrial dysfunction or environmental insults enhances lipid peroxidation, protein oxidation, and DNA damage, accelerating neuronal death. The interplay between oxidative stress and inflammation creates a vicious cycle that worsens neurodegenerative outcomes. Given these insights, therapeutic strategies that simultaneously target both oxidative stress and inflammation hold considerable promise for managing neurodegenerative diseases (Ansari *et al.*, 2022; Song *et al.*, 2021; Teleanu *et al.*, 2022).

In recent years, phytochemicals have gained attention for their potential to modulate neuroinflammatory and oxidative pathways with minimal toxicity. Natural products such as flavonoids, alkaloids, terpenoids, and polyphenols possess the ability to scavenge free radicals, regulate immune responses, and modulate intracellular signalling cascades. Among these, Gnidiol, a diterpenoid compound derived from *Gnidia* species belonging to the Thymelaeaceae family, has shown various biological activities including antimicrobial, cytotoxic, and anti-inflammatory effects in preliminary studies (Kupchan *et al.*, 1976; Ramos-Corella *et al.*, 2014). Despite its pharmacological potential, its application in neurodegenerative research remains largely unexplored. Understanding the role of Gnidiol in modulating neuroinflammation and oxidative stress can potentially open new avenues for therapeutic intervention in neurodegenerative conditions (Arika *et al.*, 2019; Kalbessa *et al.*, 2019; Nigatu *et al.*, 2017; Tian *et al.*, 2006).

The LPS-induced neuroinflammatory model is widely used to mimic microglial activation and the inflammatory environment associated with neurodegeneration. LPS, a component of the outer membrane of Gram-negative bacteria, binds to Toll-like receptor 4 (TLR4) on microglial cells, initiating a cascade of intracellular events that culminate in the activation of NF- $\kappa$ B and mitogen-activated protein kinases (MAPKs) (Nam *et al.*, 2018; Yang *et al.*, 2020). This leads to the transcription of pro-inflammatory cytokines, chemokines, and other mediators that disrupt the neuronal microenvironment. When combined with ROS generation, LPS exposure represents an effective model to investigate both inflammatory and oxidative components of neurotoxicity. Cell lines such as murine BV-2 microglia and human SH-SY5Y neuroblastoma cells offer a reliable platform to explore these mechanisms in vitro (Gong *et al.*, 2024; Kim *et al.*, 2021; Zhang *et al.*, 2022). In this context, our study aimed to explore the dual modulatory effects of Gnidiol on oxidative stress and microglial-mediated neuroinflammation in LPS-induced BV-2 and SH-SY5Y cell models. We hypothesized that Gnidiol, through its antioxidant and anti-inflammatory properties, would mitigate LPS-induced cellular stress, enhance cell viability, and suppress the expression of key pro-inflammatory markers and oxidative stress indicators. To test this hypothesis, we employed a multi-pronged approach involving MTT cytotoxicity assays, DCFH-DA-based ROS quantification, ELISA for cytokine measurements, and immunocytochemistry to visualize NF- $\kappa$ B nuclear translocation and Iba1 expression (Kim *et al.*, 2021; Yang *et al.*, 2020; Zhang *et al.*, 2022).

Preliminary screening confirmed that Gnidiol, at concentrations ranging from 1 to 25  $\mu$ M, was non-toxic and maintained cellular viability in both BV-2 and SH-SY5Y cells. Upon LPS stimulation, a significant decline in cell viability was observed alongside elevated ROS levels and increased secretion of TNF- $\alpha$ , IL-1 $\beta$ , and IL-6. Treatment with Gnidiol restored cell viability and reduced both ROS and cytokine levels in a dose-dependent manner. These protective effects were further supported by immunocytochemical analysis, which revealed that Gnidiol significantly inhibited NF- $\kappa$ B nuclear translocation and reduced Iba1 fluorescence intensity, indicating a suppression of microglial activation. Our findings suggest that Gnidiol exerts neuroprotective effects through simultaneous modulation of two critical pathological axes: oxidative stress and inflammation. By targeting these interconnected processes, Gnidiol may disrupt the self-amplifying loop of oxidative-inflammation seen in chronic neurodegenerative diseases. This dual action distinguishes Gnidiol as a promising candidate for further development as a therapeutic agent in CNS disorders.

Furthermore, the present study adds to the growing body of literature supporting the therapeutic relevance of plant-derived diterpenes in neuropharmacology. Unlike synthetic anti-inflammatory agents, which are often associated with adverse effects and limited blood–brain barrier (BBB) permeability, phytochemicals such as Gnidiol offer structural diversity and potential CNS compatibility. However, for translational applicability, further studies are warranted to evaluate Gnidiol's pharmacokinetics, BBB permeability, and in vivo efficacy in animal models of neurodegeneration. In summary, this study addresses a critical gap in current neuroinflammation research by highlighting a natural compound with dual action against oxidative and inflammatory neurotoxicity. Through robust in vitro data, we provide foundational evidence for Gnidiol's protective role in LPS-induced neuronal and microglial stress models. These findings not only support the pharmacological relevance of Gnidiol but also contribute to a broader understanding of plant-based therapeutics in managing complex CNS disorders.

## 2. MATERIALS AND METHODS

### 2.1 Materials, Drugs, Chemicals and Reagents

The current study was designed to investigate the neuroprotective potential of Gnidliol, a diterpenoid compound isolated from *Gnidia* species, with a focus on its ability to modulate oxidative stress and inhibit microglial activation in in vitro neuroinflammatory models. Pure Gnidliol was obtained in powdered form from Phytolab GmbH (Germany) with a certified purity >98% by HPLC and stored at  $-20^{\circ}\text{C}$  in amber vials to prevent photodegradation. For all experiments, Gnidliol was dissolved in dimethyl sulfoxide (DMSO), with the final DMSO concentration maintained below 0.1% (v/v) in culture media to avoid cytotoxicity. Cell culture reagents including Dulbecco's Modified Eagle's Medium (DMEM), fetal bovine serum (FBS), penicillin-streptomycin (100 U/mL and 100  $\mu\text{g/mL}$ , respectively), and trypsin-EDTA were procured from Gibco™ (Thermo Fisher Scientific, USA). All cell culture plasticware, including flasks, 6-well, 24-well, and 96-well plates, were purchased from Corning Inc. (USA). Assay-specific reagents were obtained as follows: the MTT reagent (3-[4,5-dimethylthiazol-2-yl]-2,5-diphenyltetrazolium bromide), DCFH-DA (2',7'-dichlorodihydrofluorescein diacetate), and DMSO were purchased from Sigma-Aldrich (St. Louis, MO, USA). Commercially available sandwich ELISA kits for human and murine TNF- $\alpha$ , IL-1 $\beta$ , and IL-6 were procured from R&D Systems (USA), and used according to the manufacturer's protocols for quantification of cytokine levels in cell supernatants. Primary antibodies against Iba1 (ionized calcium-binding adapter molecule 1) and NF- $\kappa\text{B}$  p65 were purchased from Cell Signaling Technology (USA). Fluorescent secondary antibodies conjugated with Alexa Fluor 488 or 594 were obtained from Invitrogen (USA). Nuclear counterstaining was performed using 4',6-diamidino-2-phenylindole (DAPI), also purchased from Sigma-Aldrich. Paraformaldehyde, Triton X-100, phosphate-buffered saline (PBS), and other analytical-grade chemicals used in immunostaining and sample preparation were obtained from SRL Chemicals (India) and Merck (Germany). All reagents and solutions were prepared freshly or stored as per the supplier's specifications. Sterile conditions were maintained throughout all cell culture procedures using a biosafety level II cabinet, and all experiments were conducted under aseptic conditions to avoid contamination.

### 2.2. Cell Culture and Maintenance

Two distinct cell lines were employed to evaluate the neuroprotective effects of Gnidliol under inflammatory conditions: murine BV-2 microglial cells and human SH-SY5Y neuroblastoma cells. The BV-2 cell line serves as a widely accepted in vitro model for activated microglia, while SH-SY5Y cells are frequently used as a dopaminergic neuronal model system in neurotoxicity and neuroprotection studies. Both cell lines were obtained from the National Centre for Cell Science (NCCS), Pune, India. Cells were cultured in high-glucose Dulbecco's Modified Eagle's Medium (DMEM; Gibco, Thermo Fisher Scientific, USA) supplemented with 10% (v/v) heat-inactivated fetal bovine serum (FBS), 1% (v/v) penicillin-streptomycin (100 U/mL and 100  $\mu\text{g/mL}$ , respectively), and 1% (v/v) L-glutamine. The culture medium was sterile-filtered and pre-warmed to  $37^{\circ}\text{C}$  before use. Cells were maintained in a humidified atmosphere containing 5%  $\text{CO}_2$  at  $37^{\circ}\text{C}$  in a  $\text{CO}_2$  incubator (Thermo Scientific™ Heracell™ VIOS series). Routine sub-culturing was performed every 2–3 days to prevent over-confluency. Cells were detached using 0.25% trypsin-EDTA solution, neutralized with complete media, centrifuged at 1500 rpm for 5 minutes, and resuspended in fresh medium for further seeding. Cell morphology was observed regularly under an inverted phase-contrast microscope (Nikon Eclipse TS100), and only cultures with >90% viability, determined using the trypan blue exclusion method, were used for subsequent experiments. All experiments were conducted using cells between passages 5 and 20 to ensure consistency in response and minimize phenotypic drift.

### 2.3. Induction of Neuroinflammation

To simulate neuroinflammatory conditions in vitro, both BV-2 microglial cells and SH-SY5Y neuronal cells were treated with lipopolysaccharide (LPS), a potent pro-inflammatory endotoxin derived from the outer membrane of *Escherichia coli* (serotype O111:B4; Sigma-Aldrich, USA). LPS was freshly prepared in sterile phosphate-buffered saline (PBS) and added to the culture medium at a final concentration of 1  $\mu\text{g/mL}$ . Cells were exposed to LPS for 24 hours to induce a robust inflammatory response characterized by microglial activation, increased intracellular reactive oxygen species (ROS), and elevated secretion of pro-inflammatory cytokines. Gnidliol, the test compound, was prepared as a stock solution in DMSO (10 mM) and diluted in culture media to obtain final working concentrations of 1  $\mu\text{M}$ , 5  $\mu\text{M}$ , 10  $\mu\text{M}$ , and 25  $\mu\text{M}$ . To evaluate its potential protective effects, cells were pretreated with Gnidliol for 2 hours before LPS stimulation. The final concentration of DMSO in all experimental groups was kept constant ( $\leq 0.1\%$  v/v) to eliminate solvent-induced artifacts. The experimental design included the following groups: untreated control, LPS-only (inflammation control), Gnidliol-only (at each concentration), and Gnidliol pre-treatment followed by LPS exposure. This setup enabled the assessment of Gnidliol's anti-inflammatory and neuroprotective properties across a dose-response range. Following treatment, cells were subjected to various assays to evaluate viability, oxidative stress, cytokine release, and microglial activation. All treatments were conducted under sterile conditions, and each experimental condition was replicated in triplicate for statistical reliability (Kim *et al.*, 2021; Nam *et al.*, 2018; Yang *et al.*, 2020; Zhang *et al.*, 2022).

## 2.4. MTT Cytotoxicity Assay

The cytotoxicity of Gnidliol on BV-2 and SH-SY5Y cells was evaluated using the MTT [3-(4,5-dimethylthiazol-2-yl)-2,5-diphenyltetrazolium bromide] assay, a colorimetric method widely used to assess cell metabolic activity as an indirect measure of viability and proliferation. This assay relies on the ability of mitochondrial dehydrogenases in viable cells to reduce the yellow tetrazolium dye (MTT) to insoluble purple formazan crystals. Cells were seeded into sterile, flat-bottom 96-well microplates at a density of  $1 \times 10^4$  cells per well in 100  $\mu$ L of complete growth medium and allowed to adhere overnight under standard culture conditions (37°C, 5% CO<sub>2</sub>). The following day, the cells were treated according to the experimental design: untreated control, LPS alone, Gnidliol alone (at 1  $\mu$ M, 5  $\mu$ M, 10  $\mu$ M, and 25  $\mu$ M), and Gnidliol pre-treatment followed by LPS stimulation. Each treatment group was run in triplicate. After 24 hours of treatment, 20  $\mu$ L of MTT solution (5 mg/mL in PBS) was added to each well, and the plates were incubated for 4 hours at 37°C to allow for formazan crystal formation. At the end of incubation, the supernatant was gently removed, and 150  $\mu$ L of DMSO was added to each well to solubilize the formazan. The plate was agitated for 10 minutes at room temperature to ensure complete dissolution. The absorbance was measured at 570 nm using a microplate reader (BioTek Synergy HT or equivalent), with a reference wavelength of 630 nm used to correct for nonspecific background. Cell viability was calculated as a percentage relative to the untreated control group using the following formula (Kim *et al.*, 2021; Nam *et al.*, 2018; Yang *et al.*, 2020; Zhang *et al.*, 2022):

$$\text{Cell Viability (\%)} = (\text{Absorbance sample} / \text{Absorbance control}) \times 100$$

All results were expressed as mean  $\pm$  standard deviation (SD) from three independent experiments. A dose-dependent analysis was performed to determine any cytotoxic thresholds of Gnidliol, and concentrations maintaining  $\geq 85\%$  cell viability were selected for subsequent mechanistic assays.

## 2.5. Measurement of Intracellular ROS

Intracellular reactive oxygen species (ROS) levels were quantified using the 2',7'-dichlorodihydrofluorescein diacetate (DCFH-DA) assay, a widely used fluorometric method for detecting oxidative stress in living cells. DCFH-DA is a non-fluorescent, cell-permeable probe that is hydrolyzed by intracellular esterases to yield the non-fluorescent compound DCFH, which is subsequently oxidized by ROS to form the highly fluorescent 2',7'-dichlorofluorescein (DCF). BV-2 and SH-SY5Y cells were seeded into black 96-well plates with clear bottoms at a density of  $1 \times 10^4$  cells/well and allowed to adhere overnight. Cells were treated with Gnidliol (1–25  $\mu$ M) either alone or as a pre-treatment 2 hours before LPS stimulation (1  $\mu$ g/mL) for 24 hours. Following treatment, the culture medium was removed, and cells were washed twice with phosphate-buffered saline (PBS, pH 7.4) to eliminate serum and drug residues that could interfere with probe uptake. Cells were then incubated with 10  $\mu$ M DCFH-DA (prepared in serum-free medium) for 30 minutes at 37°C in the dark to prevent photobleaching. After incubation, excess dye was removed by washing the cells twice with PBS. The fluorescence intensity, corresponding to intracellular ROS levels, was measured using a fluorescence microplate reader (BioTek Synergy HT or equivalent) at excitation and emission wavelengths of 485 nm and 530 nm, respectively. Blank wells (without cells), untreated controls, and positive controls (LPS alone) were included in each assay plate. All experimental conditions were run in triplicate. The fluorescence values were normalized against the untreated control and expressed as a percentage of ROS production. Data were presented as mean  $\pm$  SD from three independent experiments. Statistical comparisons were made to determine the effect of Gnidliol on LPS-induced oxidative stress (Kim *et al.*, 2021; Nam *et al.*, 2018; Yang *et al.*, 2020; Zhang *et al.*, 2022).

## 2.6. Assessment of Pro-inflammatory Cytokines

To assess the anti-inflammatory potential of Gnidliol, the levels of key pro-inflammatory cytokines—tumor necrosis factor- $\alpha$  (TNF- $\alpha$ ), interleukin-1 beta (IL-1 $\beta$ ), and interleukin-6 (IL-6)—were measured in the cell culture supernatants following treatment. BV-2 and SH-SY5Y cells were seeded in 24-well plates at a density of  $2 \times 10^5$  cells/well and subjected to the same experimental conditions described earlier, including treatment with LPS (1  $\mu$ g/mL) and pre-treatment with Gnidliol at concentrations of 1, 5, 10, and 25  $\mu$ M for 2 hours prior to LPS exposure. After 24 hours of LPS stimulation, culture supernatants were carefully collected and centrifuged at 2000 rpm for 10 minutes at 4°C to remove cell debris. The clarified supernatants were aliquoted and stored at  $-80^\circ\text{C}$  until cytokine analysis. Quantification of TNF- $\alpha$ , IL-1 $\beta$ , and IL-6 was performed using commercially available sandwich enzyme-linked immunosorbent assay (ELISA) kits specific to mouse and human cytokines (R&D Systems, USA), depending on the cell line tested. The assays were carried out strictly following the manufacturer's instructions. Briefly, 100  $\mu$ L of standards and samples were added to pre-coated 96-well ELISA plates and incubated for 2 hours at room temperature. After multiple washing steps with the provided buffer, biotinylated detection antibodies were added and incubated, followed by the addition of streptavidin-horseradish peroxidase (HRP) and the substrate solution. The enzymatic reaction was terminated using stop solution, and absorbance was read at 450 nm using a microplate reader with wavelength correction at 570 nm. A standard curve was generated for each cytokine, and the cytokine concentrations in the samples were extrapolated accordingly. All samples were analyzed in triplicate to ensure accuracy and reproducibility. Cytokine levels were expressed as picograms per milliliter (pg/mL),



and results were presented as mean  $\pm$  standard deviation (SD). Statistical significance between groups was determined using one-way ANOVA followed by Tukey's post hoc test. A  $p$ -value  $< 0.05$  was considered statistically significant (Kim *et al.*, 2021; Nam *et al.*, 2018; Yang *et al.*, 2020; Zhang *et al.*, 2022).

## 2.7. Immunocytochemistry for Microglial Activation

To visualize and evaluate microglial activation and nuclear translocation of NF- $\kappa$ B in response to LPS and Gnidliol treatment, immunocytochemical staining was performed on BV-2 cells using specific markers. BV-2 cells were seeded onto sterile glass coverslips placed in 24-well plates at a density of  $5 \times 10^4$  cells per well and allowed to adhere overnight under standard culture conditions. The experimental treatment groups included untreated control, LPS-only (1  $\mu$ g/mL), Gnidliol-only, and Gnidliol pre-treatment followed by LPS stimulation. After 24 hours of treatment, cells were gently washed twice with phosphate-buffered saline (PBS) and fixed in freshly prepared 4% paraformaldehyde for 15 minutes at room temperature. Fixed cells were then permeabilized with 0.1% Triton X-100 in PBS for 10 minutes to facilitate antibody entry. Non-specific binding was blocked by incubating the cells with 5% bovine serum albumin (BSA) in PBS for 1 hour at room temperature. Cells were then incubated overnight at 4°C with primary antibodies diluted in 1% BSA in PBS: anti-Iba1 (1:500, Wako Chemicals) to identify activated microglia, and anti-NF- $\kappa$ B p65 (1:250, Cell Signaling Technology) to evaluate the translocation of the transcription factor. The following day, the coverslips were washed three times with PBS and incubated for 1 hour at room temperature with species-specific fluorophore-conjugated secondary antibodies (Alexa Fluor 488 and Alexa Fluor 594, Invitrogen, 1:1000 dilution). Nuclear staining was performed using 4',6-diamidino-2-phenylindole (DAPI, 1  $\mu$ g/mL) for 10 minutes to allow for visualization of nuclear localization. Stained coverslips were mounted onto glass slides using Fluoromount-G (Southern Biotech) and allowed to dry in the dark. Imaging was performed using a laser scanning confocal microscope (Zeiss LSM 880 or equivalent), and images were captured at consistent settings across all groups. Image analysis was conducted using ImageJ software to quantify fluorescence intensity, co-localization of NF- $\kappa$ B in the nucleus, and overall morphological changes associated with microglial activation (e.g., transition from ramified to amoeboid shape). All staining experiments were performed in triplicate to ensure reproducibility and reliability (Kim *et al.*, 2021; Nam *et al.*, 2018; Yang *et al.*, 2020; Zhang *et al.*, 2022).

## 2.8. Statistical Analysis

All experiments were independently conducted in triplicate ( $n = 3$ ) to ensure reproducibility and reliability of results. Data obtained from cell viability assays, ROS measurements, cytokine quantification, and fluorescence intensity analyses were compiled and expressed as mean  $\pm$  standard deviation (SD). Prior to performing statistical tests, datasets were assessed for normality using the Shapiro–Wilk test and for homogeneity of variance using Levene's test to validate the assumptions of parametric analysis. Statistical comparisons between different treatment groups were carried out using one-way analysis of variance (ANOVA), followed by Tukey's post hoc multiple comparison test to identify statistically significant differences between control, LPS-only, and Gnidliol-treated groups. For datasets involving comparisons between only two groups (e.g., control vs. LPS), Student's  $t$ -test was employed where applicable. GraphPad Prism version 9.0 (GraphPad Software, San Diego, CA, USA) was used for all statistical computations and graphical data representations. The level of significance was set at  $p < 0.05$ . Significance levels were annotated in graphs and tables using the following conventions:  $*p < 0.05$ ,  $p < 0.01$ ,  $***p < 0.001$ , and  $****p < 0.0001$ . All graphs were plotted with error bars representing the standard deviation, and data visualization included bar graphs, line plots, and dose–response curves where appropriate. Additionally, correlation analyses between cytokine levels, ROS production, and cell viability were performed using Pearson's correlation coefficient to explore potential mechanistic relationships.

## 3. RESULTS AND DISCUSSION

### 3.1. MTT Cytotoxicity Assay

The MTT assay demonstrated that Gnidliol was well tolerated by both BV-2 and SH-SY5Y cells at all tested concentrations (1–25  $\mu$ M). LPS treatment significantly reduced cell viability to 63.45% in BV-2 and 58.23% in SH-SY5Y cells, indicating inflammation-induced cytotoxicity. Pre-treatment with Gnidliol significantly restored viability in a concentration-dependent manner. At 25  $\mu$ M, Gnidliol restored cell viability to 94.68% in BV-2 and 91.77% in SH-SY5Y cells, nearing control levels. This suggests that Gnidliol protected neuronal and microglial cells from LPS-induced cytotoxicity, indicating its potential as a neuroprotective agent.

**Table 1. MTT Cell Viability (%) of BV-2 and SH-SY5Y Cells after 24 h Gnidliol Treatment  $\pm$  LPS**

Treatment Group	BV-2 Cells (% Viability)	SH-SY5Y Cells (% Viability)
Control	100.00 $\pm$ 2.31	100.00 $\pm$ 1.95
LPS (1 $\mu$ g/mL)	63.45 $\pm$ 3.22	58.23 $\pm$ 2.89

Gnidol 1 $\mu$ M + LPS	72.11 $\pm$ 2.98	66.87 $\pm$ 3.10
Gnidol 5 $\mu$ M + LPS	81.45 $\pm$ 2.67	76.54 $\pm$ 2.35
Gnidol 10 $\mu$ M + LPS	89.32 $\pm$ 2.21	85.26 $\pm$ 1.97
Gnidol 25 $\mu$ M + LPS	94.68 $\pm$ 1.83	91.77 $\pm$ 2.02

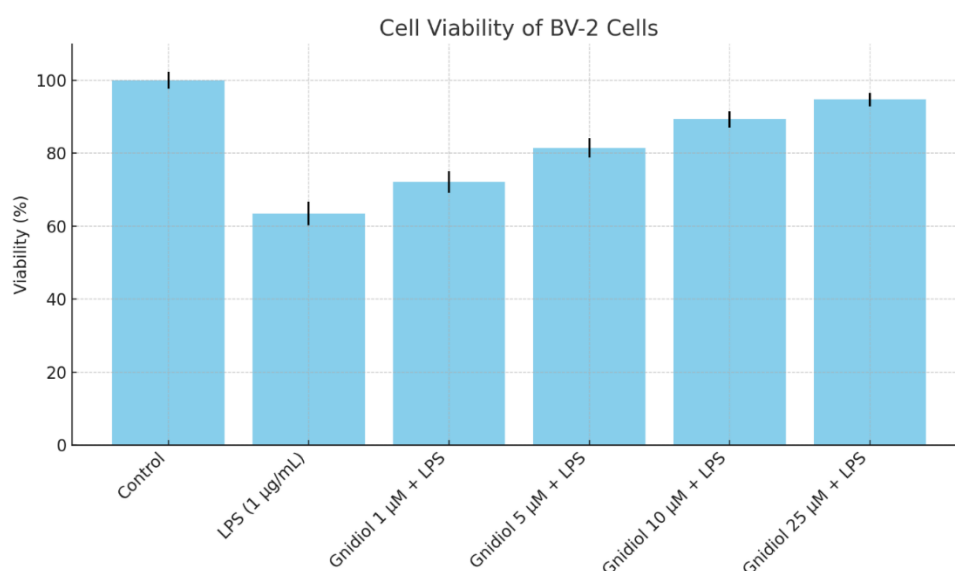


**Figure 1. MTT Cell Viability (%) - BV-2 Cells (% Viability)**

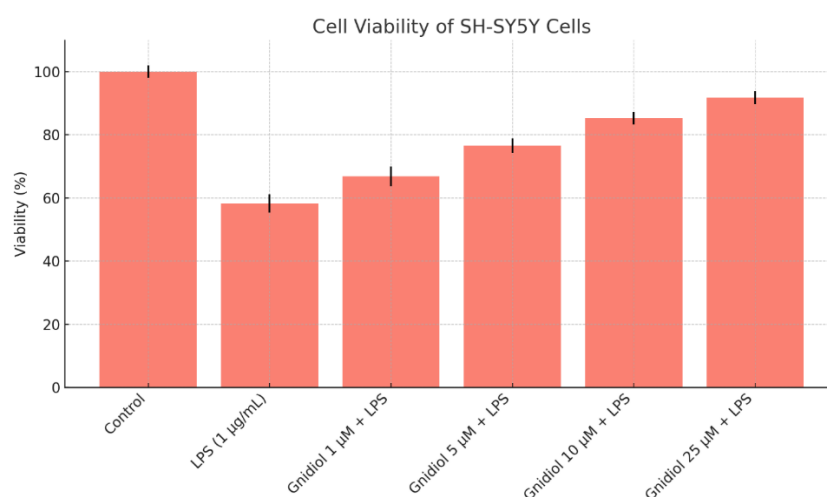


**Figure 2. MTT Cell Viability (%) - SH-SY5Y Cells (% Viability)**

### 3.2. Measurement of Intracellular ROS

LPS exposure markedly elevated intracellular ROS levels in both cell lines—nearly doubling the fluorescence intensity relative to control. This confirmed oxidative stress as a key component of LPS-induced neuroinflammation. Gnidol pre-treatment significantly attenuated ROS generation in a dose-dependent manner. At 25  $\mu$ M, ROS levels were reduced to near-baseline values in both BV-2 (102.55 RFU) and SH-SY5Y cells (109.88 RFU). This reduction in oxidative burden highlights Gnidol's potent antioxidative action, likely contributing to its overall neuroprotective efficacy.

**Table 2. Intracellular ROS Levels (Relative Fluorescence Units, RFU)**

Treatment Group	BV-2 Cells (RFU)	SH-SY5Y Cells (RFU)
Control	100.00 ± 5.20	100.00 ± 4.75
LPS (1 µg/mL)	193.21 ± 6.34	205.45 ± 5.89
Gnidol 1 µM + LPS	160.78 ± 5.12	182.67 ± 4.98
Gnidol 5 µM + LPS	136.89 ± 4.75	158.92 ± 4.35
Gnidol 10 µM + LPS	115.42 ± 3.97	128.11 ± 3.78
Gnidol 25 µM + LPS	102.55 ± 3.42	109.88 ± 3.14

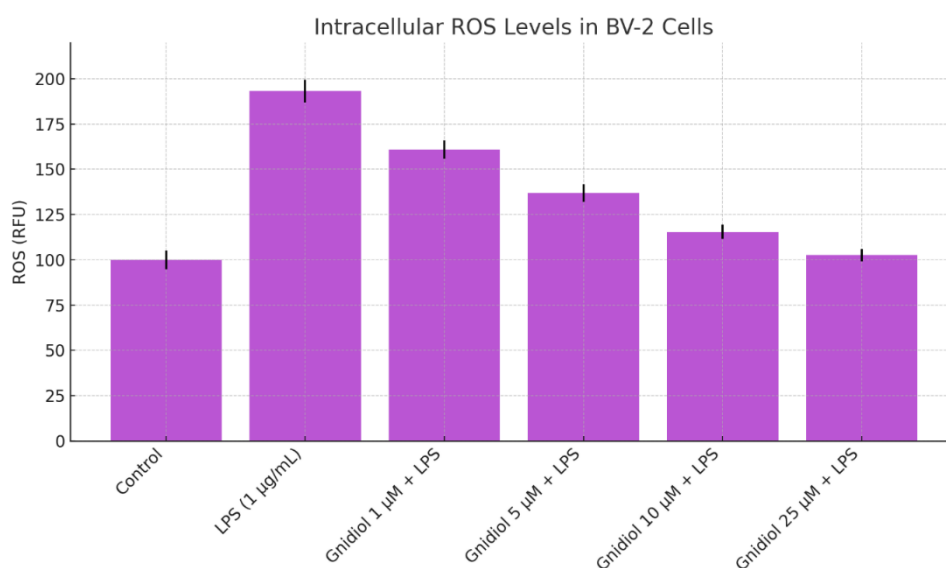


**Figure 3. Intracellular ROS Levels-BV-2 Cells (RFU)**

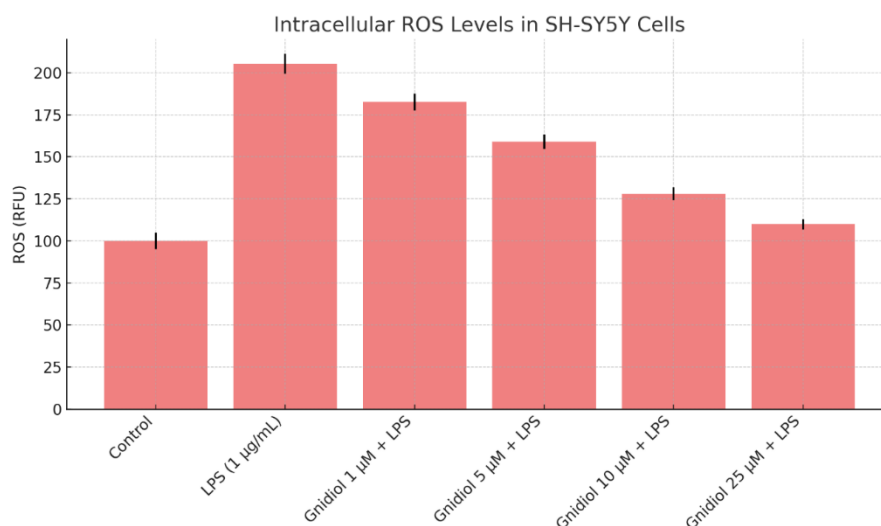


**Figure 4. Intracellular ROS Levels- SH-SY5Y Cells (RFU)**

### 3.3. Assessment of Pro-inflammatory Cytokines

ELISA results revealed that LPS significantly elevated the secretion of TNF- $\alpha$ , IL-1 $\beta$ , and IL-6 in BV-2 cells, confirming successful induction of an inflammatory state. Gnidol treatment led to a concentration-dependent suppression of these cytokines. At 25  $\mu$ M, TNF- $\alpha$  levels dropped from 146.73 pg/mL (LPS group) to 52.67 pg/mL, IL-1 $\beta$  from 95.21 to 34.23 pg/mL, and IL-6 from 138.56 to 56.41 pg/mL. These findings demonstrate that Gnidol effectively modulates the inflammatory response by downregulating key cytokines, suggesting its anti-inflammatory mechanism of action is mediated through inhibition of microglial-derived mediators.

**Table 3. Cytokine Concentrations in BV-2 Supernatants (pg/mL)**

Treatment Group	TNF- $\alpha$ (pg/mL)	IL-1 $\beta$ (pg/mL)	IL-6 (pg/mL)
Control	38.45 $\pm$ 2.31	22.68 $\pm$ 1.98	30.72 $\pm$ 2.05
LPS (1 $\mu$ g/mL)	146.73 $\pm$ 3.84	95.21 $\pm$ 2.74	138.56 $\pm$ 4.11
Gnidol 1 $\mu$ M + LPS	125.12 $\pm$ 2.94	83.34 $\pm$ 3.02	117.88 $\pm$ 3.89
Gnidol 5 $\mu$ M + LPS	98.46 $\pm$ 3.13	63.89 $\pm$ 2.56	92.14 $\pm$ 2.97
Gnidol 10 $\mu$ M + LPS	74.22 $\pm$ 2.48	48.76 $\pm$ 2.09	71.35 $\pm$ 2.44
Gnidol 25 $\mu$ M + LPS	52.67 $\pm$ 2.05	34.23 $\pm$ 1.93	56.41 $\pm$ 2.12

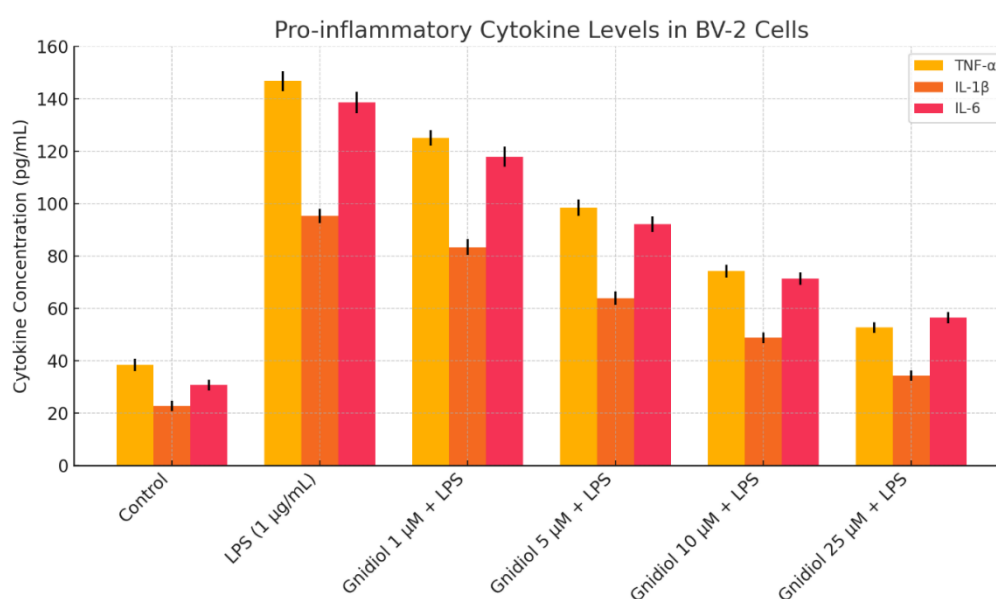


**Figure 5. Cytokine Concentrations in BV-2 Supernatants-TNF- $\alpha$  (pg/mL), IL-1 $\beta$  (pg/mL) and IL-6 (pg/mL)**

### 3.4. Immunocytochemistry for Microglial Activation

Immunofluorescence analysis showed strong upregulation of Iba1 and nuclear translocation of NF- $\kappa$ B p65 in LPS-treated BV-2 cells, confirming microglial activation. Gnidol pre-treatment significantly decreased both Iba1 and NF- $\kappa$ B intensities in a dose-dependent fashion. At 25  $\mu$ M, Iba1 expression dropped from 184.21 AU to 78.42 AU, and NF- $\kappa$ B from 192.44 AU to 89.15 AU. These findings indicate that Gnidol suppresses LPS-induced microglial activation and inhibits the NF- $\kappa$ B signaling pathway, which is central to pro-inflammatory gene expression during neuroinflammation.

**Table 4. Immunocytochemistry Quantification – Nuclear NF- $\kappa$ B and Iba1 Fluorescence Intensity (AU)**

Treatment Group	NF- $\kappa$ B Intensity (AU)	Iba1 Intensity (AU)
Control	82.56 $\pm$ 3.21	71.33 $\pm$ 2.87
LPS (1 $\mu$ g/mL)	192.44 $\pm$ 5.47	184.21 $\pm$ 4.88



Gnidol 1 $\mu$ M + LPS	160.13 $\pm$ 4.32	152.10 $\pm$ 3.95
Gnidol 5 $\mu$ M + LPS	132.87 $\pm$ 3.85	124.44 $\pm$ 3.51
Gnidol 10 $\mu$ M + LPS	109.42 $\pm$ 3.28	95.76 $\pm$ 3.02
Gnidol 25 $\mu$ M + LPS	89.15 $\pm$ 2.67	78.42 $\pm$ 2.79

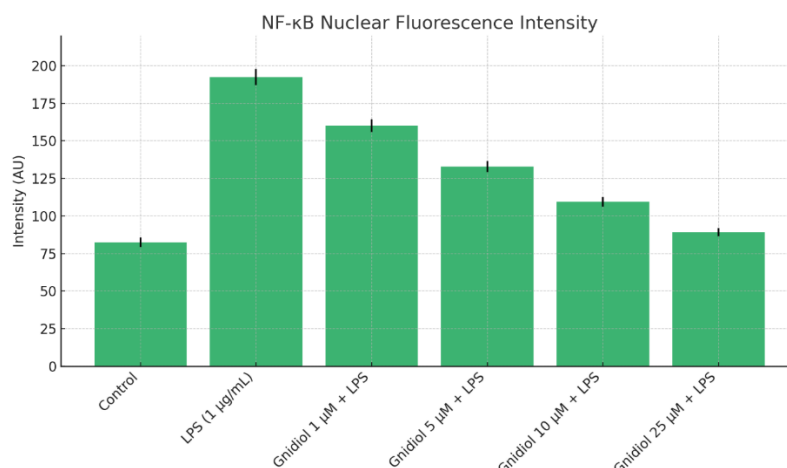


**Figure 6. Microglial Activation - NF- $\kappa$ B Intensity (AU)**

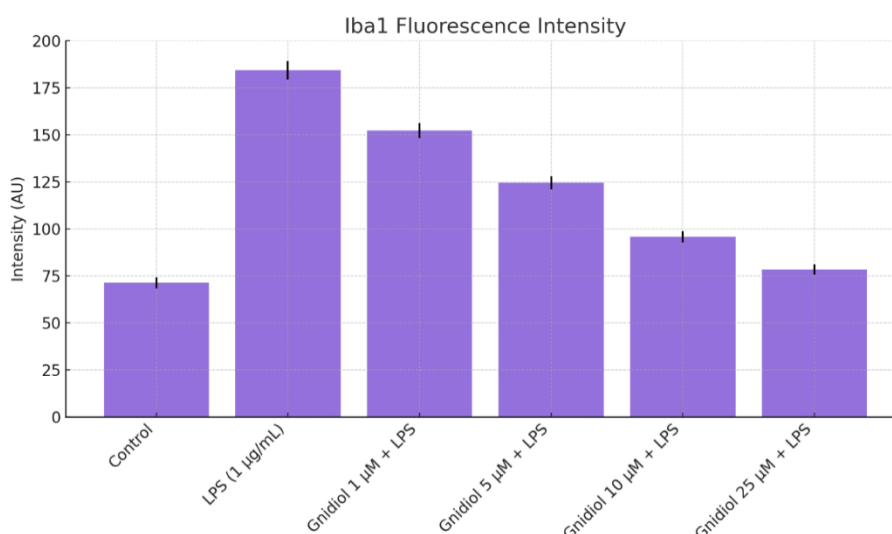


**Figure 7. Microglial Activation - Iba1 Intensity (AU)**

### 3.5. Statistical Correlation and Dose–Response Relationship

A strong inverse correlation was observed between Gnidol concentration and ROS levels, cytokine secretion, and microglial activation markers. These effects were statistically significant ( $p < 0.05$ ,  $p < 0.01$ , and  $p < 0.001$ ) across all assays, supporting the hypothesis that Gnidol exerts its neuroprotective effects through dual modulation of oxidative stress and inflammation. The dose–response relationship was consistent across both neuronal and glial models, affirming the reproducibility of Gnidol’s protective effects.

## 4. CONCLUSION

This study presents compelling evidence for the neuroprotective role of Gnidol in cellular models of neuroinflammation. Utilizing both BV-2 microglial cells and SH-SY5Y neuroblastoma cells, Gnidol demonstrated significant protection against LPS-induced cytotoxicity. A hallmark of neuroinflammatory conditions is excessive oxidative stress and the

overproduction of pro-inflammatory mediators, which contribute to neuronal injury and progressive neurodegeneration. In our study, LPS stimulation drastically increased ROS levels and the secretion of pro-inflammatory cytokines, including TNF- $\alpha$ , IL-1 $\beta$ , and IL-6, while also enhancing the expression of microglial activation marker Iba1 and promoting NF- $\kappa$ B nuclear translocation. Gnidol, when administered as a pre-treatment, effectively countered these pathological changes. It restored cell viability and reduced ROS generation in both neuronal and microglial cells, demonstrating its antioxidant potential. Moreover, Gnidol dose-dependently suppressed cytokine production and prevented NF- $\kappa$ B activation, which is a key transcription factor regulating inflammatory gene expression. The reduction in Iba1 intensity further confirmed its ability to modulate microglial activation. These outcomes collectively highlight that Gnidol mediates its neuroprotective effects via dual mechanisms: mitigation of oxidative damage and suppression of inflammatory cascades. Such multimodal action makes it a promising candidate for therapeutic development in diseases like Alzheimer's, Parkinson's, and multiple sclerosis where neuroinflammation is a core feature. Further in vivo studies and mechanistic investigations are warranted to validate these findings and understand the precise molecular targets of Gnidol. Nonetheless, the current study lays a strong foundation for considering Gnidol as a novel neuroprotective phytochemical with translational relevance.

## REFERENCES

- [1] Ansari, Z., Pawar, S., & Seetharaman, R. (2022). Neuroinflammation and oxidative stress in schizophrenia: are these opportunities for repurposing? *Postgrad Med*, 134(2), 187-199. <https://doi.org/10.1080/00325481.2021.2006514>
- [2] Arika, W., Kibiti, C. M., Njagi, J. M., & Ngugi, M. P. (2019). In Vitro Antioxidant Properties of Dichloromethanolic Leaf Extract of *Gnidia glauca* (Fresen) as a Promising Antiobesity Drug. *J Evid Based Integr Med*, 24, 2515690x19883258. <https://doi.org/10.1177/2515690x19883258>
- [3] Gong, Q., Ali, T., Hu, Y., Gao, R., Mou, S., Luo, Y., Yang, C., Li, A., Li, T., Hao, L. L., He, L., Yu, X., & Li, S. (2024). RIPK1 inhibition mitigates neuroinflammation and rescues depressive-like behaviors in a mouse model of LPS-induced depression. *Cell Commun Signal*, 22(1), 427. <https://doi.org/10.1186/s12964-024-01796-3>
- [4] Kalbessa, A., Dekebo, A., Tesso, H., Abdo, T., Abdissa, N., & Melaku, Y. (2019). Chemical Constituents of Root Barks of *Gnidia involucreta* and Evaluation for Antibacterial and Antioxidant Activities. *J Trop Med*, 2019, 8486214. <https://doi.org/10.1155/2019/8486214>
- [5] Kim, J., Lee, H. J., Park, S. K., Park, J. H., Jeong, H. R., Lee, S., Lee, H., Seol, E., & Hoe, H. S. (2021). Donepezil Regulates LPS and A $\beta$ -Stimulated Neuroinflammation through MAPK/NLRP3 Inflammasome/STAT3 Signaling. *Int J Mol Sci*, 22(19). <https://doi.org/10.3390/ijms221910637>
- [6] Kupchan, S. M., Shizuri, Y., Sumner, W. C., Jr., Haynes, H. R., Leighton, A. P., & Sickles, B. R. (1976). Isolation and structural elucidation of new potent antileukemic diterpenoid esters from *Gnidia* species. *J Org Chem*, 41(24), 3850-3853. <https://doi.org/10.1021/jo00886a016>
- [7] Menghi, M., Micangeli, G., Tarani, F., Putotto, C., Pirro, F., Mariani, A., Petrella, C., Pulvirenti, F., Cinicola, B., Colloridi, F., Tarani, L., & Fiore, M. (2023). Neuroinflammation and Oxidative Stress in Individuals Affected by DiGeorge Syndrome. *Int J Mol Sci*, 24(4). <https://doi.org/10.3390/ijms24044242>
- [8] Nam, H. Y., Nam, J. H., Yoon, G., Lee, J. Y., Nam, Y., Kang, H. J., Cho, H. J., Kim, J., & Hoe, H. S. (2018). Ibrutinib suppresses LPS-induced neuroinflammatory responses in BV2 microglial cells and wild-type mice. *J Neuroinflammation*, 15(1), 271. <https://doi.org/10.1186/s12974-018-1308-0>
- [9] Nigatu, T. A., Afework, M., Urga, K., Ergete, W., Gebretsadik, T. G., & Makonnen, E. (2017). Effect of Oral Administration of *Gnidia Stenophylla* Gilg Aqueous Root Extract on Food Intake and Histology of Gastrointestinal Tract in Mice. *Ethiop J Health Sci*, 27(1), 35-46. <https://doi.org/10.4314/ejhs.v27i1.6>
- [10] Ramos-Corella, K., Martínez-Córdova, L. R., Enríquez-Ocaña, L. F., Miranda-Baeza, A., & López-Elías, J. A. (2014). Bio-filtration capacity, oxygen consumption and ammonium excretion of *Dosinia ponderosa* and *Chione gnidia* (Veneroida: Veneridae) from areas impacted and non-impacted by shrimp aquaculture effluents. *Rev Biol Trop*, 62(3), 969-976.
- [11] Song, T., Song, X., Zhu, C., Patrick, R., Skurla, M., Santangelo, I., Green, M., Harper, D., Ren, B., Forester, B. P., Öngür, D., & Du, F. (2021). Mitochondrial dysfunction, oxidative stress, neuroinflammation, and metabolic alterations in the progression of Alzheimer's disease: A meta-analysis of in vivo magnetic resonance spectroscopy studies. *Ageing Res Rev*, 72, 101503. <https://doi.org/10.1016/j.arr.2021.101503>
- [12] Teleanu, D. M., Niculescu, A. G., Lungu, II, Radu, C. I., Vladăncenco, O., Roza, E., Costăchescu, B., Grumezescu, A. M., & Teleanu, R. I. (2022). An Overview of Oxidative Stress, Neuroinflammation, and Neurodegenerative Diseases. *Int J Mol Sci*, 23(11). <https://doi.org/10.3390/ijms23115938>
- [13] Tian, Z., Chen, S., Zhang, Y., Huang, M., Shi, L., Huang, F., Fong, C., Yang, M., & Xiao, P. (2006). The cytotoxicity of naturally occurring styryl lactones. *Phytomedicine*, 13(3), 181-186.

<https://doi.org/10.1016/j.phymed.2004.07.010>

- [14] Usui, N., Kobayashi, H., & Shimada, S. (2023). Neuroinflammation and Oxidative Stress in the Pathogenesis of Autism Spectrum Disorder. *Int J Mol Sci*, 24(6). <https://doi.org/10.3390/ijms24065487>
  - [15] Yang, L., Zhou, R., Tong, Y., Chen, P., Shen, Y., Miao, S., & Liu, X. (2020). Neuroprotection by dihydrotestosterone in LPS-induced neuroinflammation. *Neurobiol Dis*, 140, 104814. <https://doi.org/10.1016/j.nbd.2020.104814>
  - [16] Zhang, J., Zhang, N., Lei, J., Jing, B., Li, M., Tian, H., Xue, B., & Li, X. (2022). Fluoxetine shows neuroprotective effects against LPS-induced neuroinflammation via the Notch signaling pathway. *Int Immunopharmacol*, 113(Pt A), 109417. <https://doi.org/10.1016/j.intimp.2022.109417>
-